

## 2-D deconvolution imaging condition for shot-profile migration

Alejandro A. Valenciano\* and Biondo Biondi, Stanford University

### SUMMARY

A significant improvement of seismic image resolution can be obtained by setting the shot-profile migration imaging condition as a 2-D deconvolution in the shot position-time dimension  $(x_s, t)$  domain.

### INTRODUCTION

Shot-profile migration is a method used to construct an image of the earth interior from seismic data. This technique is implemented in two steps. The first step, consist in constructing the source and receiver wavefield for each shot position, and the second step, consist in applying the imaging condition. The imaging step is based on Claerbout's imaging principle (Claerbout, 1971).

A practical way to implement Claerbout's imaging principle is by using match filters (crosscorrelation of the shot and receiver wavefields). Therefore, for each shot position, a partial image is obtained by matching the source and the receiver wavefields along the time dimension. Then, the image is form stacking the partial images.

We propose a different imaging condition that is based on Claerbout's imaging principle. It consist in deconvolving the receiver wavefield by the source wavefield in two dimensions  $(x_s, t)$ . This imaging condition satisfies Claerbout's imaging principle (Claerbout, 1971). It also improves the resolution of the image and reduces illumination effects in the final the image.

In this paper we show the advantages of the 2-D deconvolution over the crosscorrelation and the 1-D deconvolution imaging conditions. This model consists in four reflectors dipping pinching-out. There, we demonstrate the advantages of 2-D deconvolution for image resolution.

### DATA AND WAVEFIELDS DIMENSIONALITY

To implement a better imaging condition that is feasible in practice it is important to understand the 3-D prestack data and wavefields dimensionality. 3-D prestack seismic data is defined in a 5-D continuum  $(t, x_s, y_s, x_g, y_g)$  (Biondi, 1998), where  $t$  is time,  $x_s$  is the source  $x$  position,  $y_s$  is the source  $y$  position,  $x_g$  is the geophone  $x$  position, and  $y_g$  is the geophone  $y$  position. After applying the first step of shot-profile migration (source and receiver wavefields construction) we have for each shot position  $(x_s, y_s)$  the source and the receiver wavefields  $\mathbf{u}(x, y, z, t)$  and  $\mathbf{d}(x, y, z, t)$ . After wavefields propagation a new dimension is added ( $z$ ). Then the wavefields have 6-D dimensions.

In the following analysis we explain how to combine the source and the receiver wavefields to obtain an image. To make it easier we restrict our analysis to 2-D prestack data. Thus the source and receiver wavefields are 4-D datasets defined in  $(x, z, t)$  for each shot position  $x_s$ .

### 1-D IMAGING CONDITIONS

#### Claerbout's imaging principle

According to Claerbout (1971) imaging principle, a reflector exists at a point where the source and the receiver wavefields coincide in time and space. Claerbout (1971) expresses the imaging condition as follows:

$$\mathbf{r}(x, z) = \frac{\mathbf{u}(x, z, t_d)}{\mathbf{d}(x, z, t_d)}, \quad (1)$$

where  $x$  is the horizontal coordinate,  $z$  is the depth, and  $t_d$  is the

time at which the source wavefield  $\mathbf{d}(x, z, t_d)$  and the receiver wavefield  $\mathbf{u}(x, z, t_d)$  coincide in time and space. This principle states that the reflectivity strength  $\mathbf{r}(x, z)$  depends only on the source wavefield and on the receiver wavefield at time  $t_d$ .

We don't know a priori the time  $t_d$ , thus we need a practical way to locate the reflector position in  $(x, z)$  plane and compute its strength.

#### 1-D Crosscorrelation

A practical way to compute the reflectivity strength is discussed in Claerbout's paper (Claerbout, 1971). He computes the reflector strength and position as the zero lag of the crosscorrelation of the source and receiver wavefields in the time dimension (Figure 1).

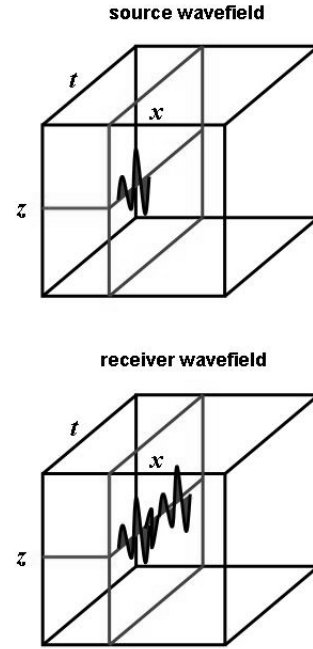


Figure 1: Source and receiver wavefields to match in the time dimension.

This is expressed in the formula :

$$\mathbf{r}(x, z) = \sum_{x_s} \sum_{\omega} \mathbf{U}(x, z, \omega, x_s) \mathbf{D}^*(x, z, \omega, x_s), \quad (2)$$

where  $\mathbf{r}(x, z)$  is the zero lag coefficient of the crosscorrelation, that is computed summing over the frequencies.  $\mathbf{U}(x, z, \omega)$  and  $\mathbf{D}(x, z, \omega)$  are the one dimensional Fourier Transforms of the receiver and source wavefields respectively. The contribution of each shot (located at  $x_s$ ) is added to form the final image.

#### 1-D Deconvolution

The imaging condition can be extended beyond a simple crosscorrelation by implementing a 1-D deconvolution (in the time dimension), adding more complexity to honor the physics of reflection as

## 2-D deconvolution imaging condition

stated in:

$$\mathbf{r}(x, z) = \sum_{x_s} \sum_{\omega} \frac{\mathbf{U}(x, z, \omega, x_s) \mathbf{D}^*(x, z, \omega, x_s)}{\mathbf{D}(x, z, \omega, x_s) \mathbf{D}^*(x, z, \omega, x_s) + \varepsilon^2(x, z, x_s)}. \quad (3)$$

Notice that  $\varepsilon(x, z, x_s)$  is variable (even in the  $(x_s, t)$  plane). It is calculated as

$$\varepsilon^2(x, z, x_s) = \lambda \langle \mathbf{D}(x, z, \omega, x_s) \mathbf{D}^*(x, z, \omega, x_s) \rangle \quad (4)$$

where  $\langle \rangle$  means the mean.

### 2-D IMAGING CONDITIONS IN THE $(X_S, T)$ DIMENSIONS

Another practical way of computing the reflectivity strength can be by applying the imaging condition, 2-D crosscorrelation or 2-D deconvolution, in the shot position time dimensions  $(x_s, t)$ . Figure 2 shows the domain where this operations should be done. For a fix  $(x, z)$  position in the image there is a plane with dimensions  $(x_s, t)$ .

#### 2-D crosscorrelation

It turns out that the zero lag of the 2-D crosscorrelation of the source and the receiver wavefields in  $(x_s, t)$  give the same result that taking the zero lag of the 1-D crosscorrelation in the time domain and stacking through the shot position dimension. A simple example with matrices illustrates the concept. If we 2-D crosscorrelate 2 matrices,

$$\begin{bmatrix} 1 & 2 \\ 2 & 3 \end{bmatrix} \star \star \begin{bmatrix} 4 & 1 \\ 2 & 5 \end{bmatrix} = \begin{bmatrix} 5 & 12 & 4 \\ 11 & 25 & 14 \\ 2 & 11 & 12 \end{bmatrix}, \quad (5)$$

and take the zero lag the result is 25. Now if we crosscorrelate the columns,

$$\begin{bmatrix} 1 \\ 2 \end{bmatrix} \star \begin{bmatrix} 4 \\ 2 \end{bmatrix} = \begin{bmatrix} 2 \\ 8 \\ 8 \end{bmatrix} \quad (6)$$

$$\begin{bmatrix} 2 \\ 3 \end{bmatrix} \star \begin{bmatrix} 1 \\ 5 \end{bmatrix} = \begin{bmatrix} 10 \\ 17 \\ 3 \end{bmatrix} \quad (7)$$

take the zero lag and stack in the raws direction the result is also 25.

#### 2-D deconvolution

In the case of deconvolution the relation between 2-D and 1-D (plus stacking), if exists, is not straightforward to show, because deconvolution in the space domain is implemented by recursive filtering. But, we know that 2-D deconvolution in the  $(x_s, t)$  plane compresses the information in both shot and the time dimensions. This is a better way of compressing than information 1-D deconvolution.

For the 2-D deconvolution, we can state the following imaging condition:

$$\mathbf{r}(x, z) = \sum_{k_{x_s}} \sum_{\omega} \frac{\mathbf{U}(x, z, \omega, k_{x_s}) \mathbf{D}^*(x, z, \omega, k_{x_s})}{\mathbf{D}(x, z, \omega, k_{x_s}) \mathbf{D}^*(x, z, \omega, k_{x_s}) + \varepsilon^2(x, z)} \quad (8)$$

where  $\mathbf{r}(x, z)$  is the zero lag of the 2-D deconvolution computed as the sum over temporal frequency ( $\omega$ ) and shot position frequency ( $k_{x_s}$ ).  $\mathbf{U}(x, z, \omega, k_{x_s})$  and  $\mathbf{D}(x, z, \omega, k_{x_s})$  are the two dimensional Fourier transforms of the receiver and source wavefields respectively. Notice that  $\varepsilon(x, z)$  is variable but constant in  $(x_s, t)$  plane and is calculated as

$$\varepsilon^2(x, z) = \lambda \langle \mathbf{D}(x, z, \omega, k_{x_s}) \mathbf{D}^*(x, z, \omega, k_{x_s}) \rangle \quad (9)$$

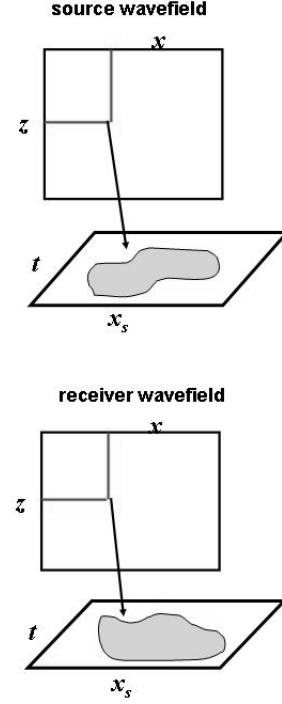


Figure 2: Source and receiver wavefields to match in the time shot position dimensions.

where  $\langle \rangle$  means the mean.

We have change a 1-D deconvolution in time and stacking in the shot position direction by a 2-D deconvolution in the  $(x_s, t)$  plane. The 2-D deconvolution imaging condition gives a better resolution image as we show with the following example.

### RESULTS WITH SYNTHETIC DATA

To test the previous idea we build a constant velocity model of five dipping layers pinching-out to the right of the model. The deepest reflector has the steepest angle ( $\approx 63^\circ$ ) and the shallower has zero dip. Figure 3 shows a comparison of three different imaging conditions. Figure 3(a) is the image obtained with the crosscorrelation imaging condition, Figure 3(b) is the image obtained with the 1-D deconvolution imaging condition (time dimension) and Figure 3(c) is the image obtained with the 2-D deconvolution imaging condition in the  $(x_s, t)$  dimensions. Figure 4 shows a close-up of Figure 3 in the pinch-out region. Notice the better resolution of the 2-D deconvolution image.

The better resolution of the 2-D deconvolution image is corroborated comparing Figure 5 and Figure 6. They show the result of 1-D deconvolution and 2-D deconvolution for different  $\lambda$  values at a fixed  $x$  position (1.96 Km). Notice that when  $\lambda$  decreases the 1-D deconvolution result presents low frequency noise. In the case of 2-D deconvolution when  $\lambda$  decreases the random noise contaminates the image.

After this comparison we can see that the 2-D deconvolution imaging condition in the  $(x_s, t)$  dimensions gives a better resolution than the other imaging conditions. The image, in this case, has more

## 2-D deconvolution imaging condition

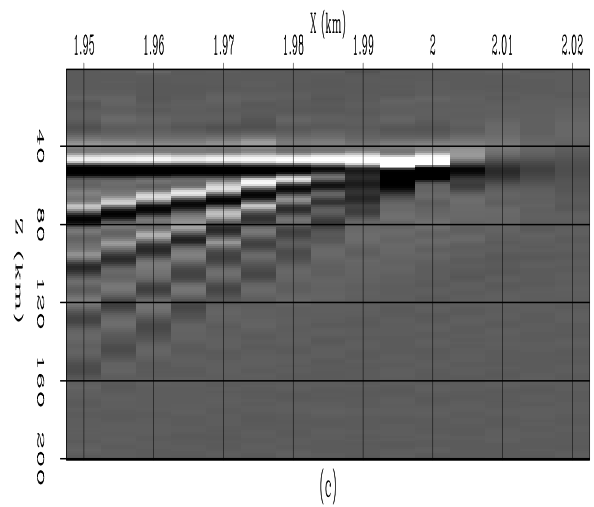
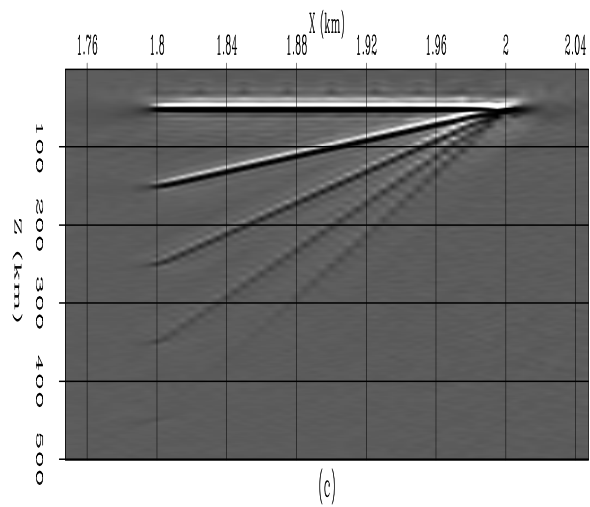
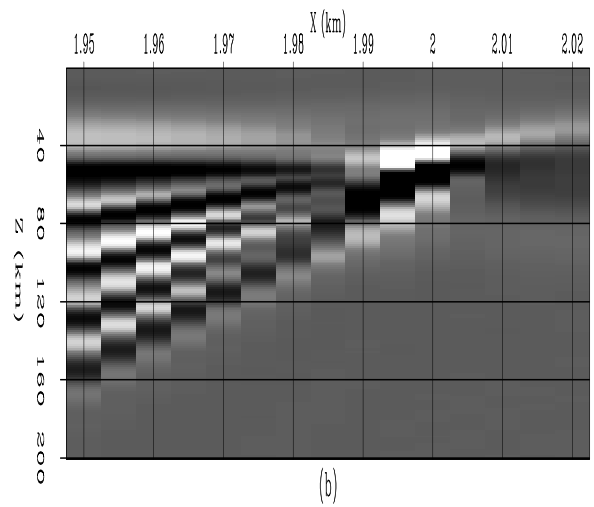
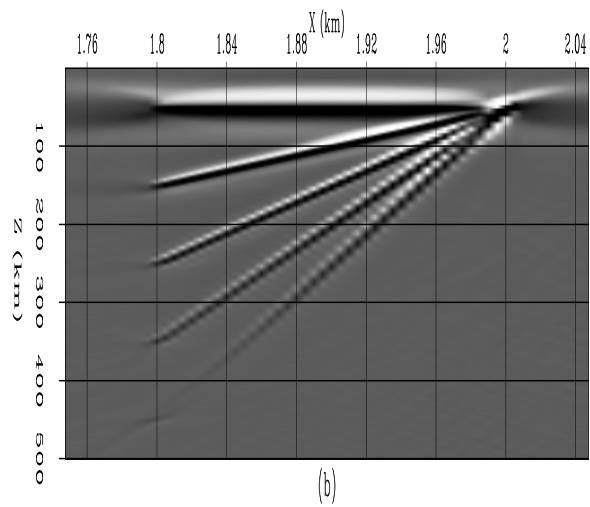
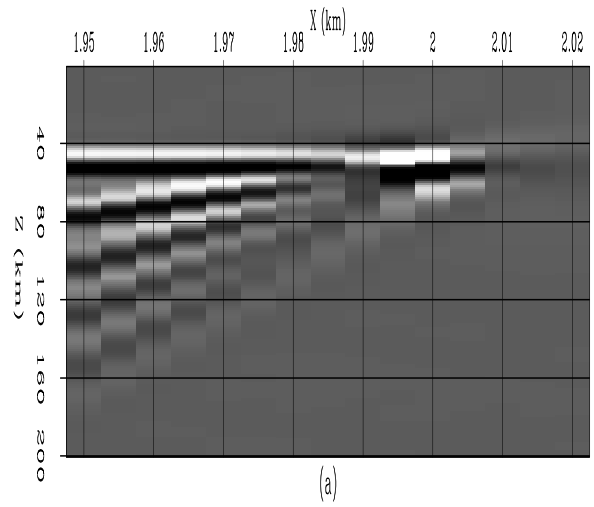
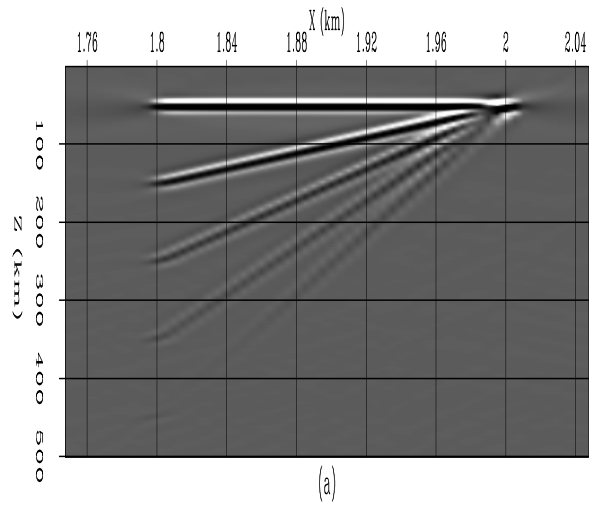


Figure 3: Comparison of 3 different imaging conditions.(a) image obtained with the crosscorrelation imaging condition, (b) image obtained with the 1-D deconvolution imaging condition (time dimension) and (c) image obtained with the 2-D deconvolution imaging condition in the  $(x_s, t)$  dimensions.

Figure 4: Zoom of Figure 3 in the pinch-out region. (a) image obtained with the crosscorrelation imaging condition, (b) image obtained with the 1-D deconvolution imaging condition (time dimension) and (c) image obtained with the 2-D deconvolution imaging condition in the  $(x_s, t)$  dimensions.

## 2-D deconvolution imaging condition

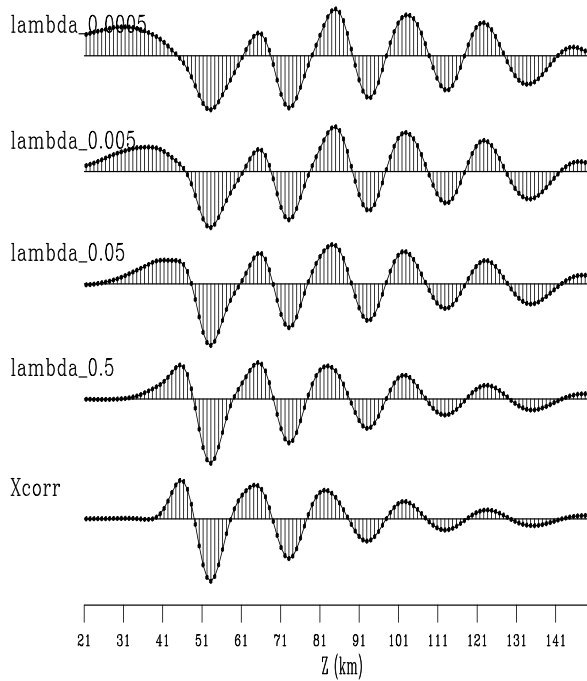


Figure 5: Effect of lambda value on 1-D deconvolution. From bottom to top: crosscorrelation,  $\lambda = 0.5$ ,  $\lambda = 0.05$ ,  $\lambda = 0.005$  and  $\lambda = 0.0005$

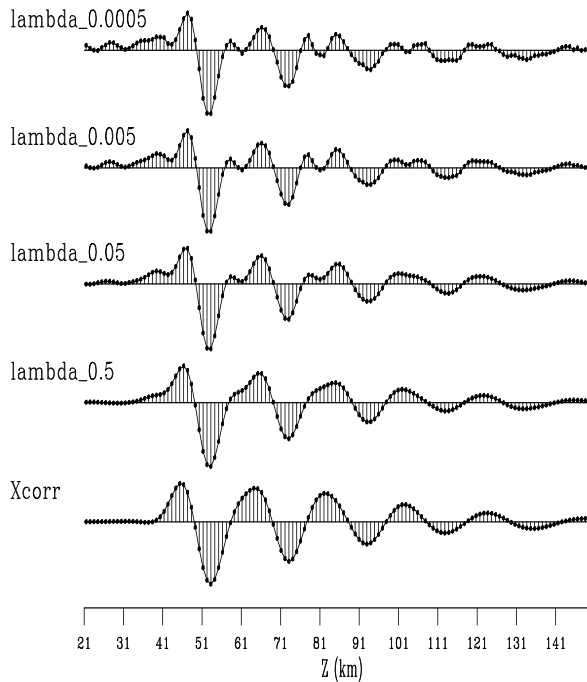


Figure 6: Effect of lambda value on 2-D deconvolution. From bottom to top: crosscorrelation,  $\lambda = 0.5$ ,  $\lambda = 0.05$ ,  $\lambda = 0.005$  and  $\lambda = 0.0005$

random noise but this is a manifestation of the well known trade off effect between signal to noise ratio and resolution.

## CONCLUSIONS

Implementing the shot-profile migration imaging condition as a 2-D deconvolution in the  $(x_s, t)$  plane leads to a better image resolution. This implementation has the advantage of not stacking in the shot position dimension thus increasing resolution.

## ACKNOWLEDGMENTS

The authors want to thanks Goijan Shan and Brad Artman for providing the programs to construct the source and receiver wavefields. We also thanks Paul Sava, Antoine Guitton and Gabriel Alvarez for their important suggestions.

## REFERENCES

- Biondi, B., 1998, 3-D seismic imaging: SEP-98, 1-204.
- Claerbout, J. F., 1971, Toward a unified theory of reflector mapping: Geophysics, 36, no. 3, 467-481.